# Experimental study of the turbulent structure of a boundary layer developing over a rough surface

**S. TOMAS**[a,b], **O. EIFF**[c], **V. MASSON**[b]

*a. Centre National de Recherches Météorologiques, CNRM-GAME (URA1357), Météo-France/CNRS, Toulouse, France. TOULOUSE*
*b. Current affiliation : Cemagref, UMR G-EAU/LERMI, AIX EN PROVENCE*
*c. Institut de Mécanique des Fluides de Toulouse - Université de Toulouse, TOULOUSE*

## Résumé :

*Nous avons analysé les caractéristiques turbulentes de la couche limite neutre se développant sur une surface rugueuse. Des expériences ont été réalisées dans un canal hydraulique pour mesurer les champs bidimensionnels de vitesse via la technique de Particle Image Velocimetry (PIV). Ces données expérimentales décrivent cette couche limite en termes de quantités moyennes et turbulentes avec un haut niveau de précision. Les termes des budgets d'énergie ont ainsi pu être estimés. Il apparait que le développement de la couche limite rugueuse ne modifie pas significativement la répartition entre les termes constitutifs des différents bilans. Les échelles de longueurs intégrales ont été estimées, de manière directe, à partir des corrélations spatiales. Ces échelles de longueurs verticales permettent alors de paramétrer les longueurs de mélange et de dissipation, utilisées dans des modèles 1D de prédiction.*

## Abstract :

*We analyzed the turbulent characteristics of the neutral boundary-layer developing over rough surfaces. A set of hydraulic flume experiments were carried out in order to measure two-dimensional velocity fields via a particle image velocimetry (PIV) technique. The resulting experimental data describe this boundary layer in terms of the mean and turbulent quantities with a high level of accuracy. These results enabled the terms of the energy budgets to be estimated and show that the development of the rough neutral boundary layer does not significantly modify the repartition between the constitutive terms of the different budget. Spatial correlation analysis permitted the longitudinal and vertical integral length also to be estimated directly. Theses vertical length scales are then used to parameterize the mixing and dissipative lengths, used in 1D prediction models.*

**Mots clefs : rough turbulent boundary-layer, turbulent budgets, integral scales, mixing length parameterization**

## 1 Introduction

Townsend's (1976) similarity hypothesis stipulates that at high Reynolds numbers the turbulent flow outside the near-wall region is independent of the wall roughness. Some studies agree but other suggest that the roughness tends to produce dynamic effects across the boundary-layer depth (Antonia and Krogstad, 2001 ; Coceal et al., 2006). In view of reconciliations, Jiménez (2004) suggested that two dimensionless parameters, the roughness Reynolds number ($Re_* = z_h u_*/\nu$ where $u_*$ is the friction velocity and $z_h$ is the roughness height) and the blockage ratio ($\delta/z_h$ where $\delta$ is the boundary-layer thickness), control the effect of rough walls on turbulent boundary-layers. In support, recent measurements of Schultz and Flack (2007) at high Reynolds number and small blockage ratio show that the mean flow and turbulent profiles are self similar. They argue that at least some of the observed discrepancies can be attributed to non-sufficiently high Reynolds numbers and/or too high blockage ratios. Castro (2007), however suggests that similarity, at least for the mean flow, is achieved for much lower blockage ratio ($\delta/z_h$ >5). So, while there might still be questions concerning similarity, all these studies dealt with (rough) boundary layer at the equilibrium. Castro (2007) reexamined data to evaluate the mean flow development but did not consider the turbulent statistics and budgets. Here, we investigate the development of a boundary layer over rough surface, also at high Reynolds number and low blockage ratio with the aim to evaluate the development of turbulent statistics above the surface layer of a fully rough developing neutral boundary layer. The turbulent energy budgets and transfers between Reynolds stresses in the outer layer are also computed and discussed. Finally, the computation of the spatial integral scales leads to a proposition for the parameterizations of the dissipative and mixing length scales.

## 2 Experimental procedure

The experiments were carried out in a large hydraulic flume (22m long, 3m wide and 1m high) to obtain high Reynolds numbers ($Re_\delta \sim 4000$) and low blockage ratio (3%). It was equipped with a series of grids to reduce the turbulence intensity and homogenize the incident flow. A one meter smooth surface behind the last grid was chosen to allow a uniform flow with a low level of turbulence and a small boundary layer to approach the roughness elements. The boundary layer was then allowed to develop over a horizontal rough surface 12.3m long. The roughness elements are constituted by LEGO© blocks (3.17×1.57×0.96cm) to create a turbulent flow in the canopy ($Re_* \sim 200$). The arrangement was chosen to represent a medium roughness length corresponding to open fields (plan area density : $\lambda_p = 0.5$ and frontal area density : $\lambda_f = 0.2$ ; MacDonald, 2000).

The PIV experiments were performed at two different free-stream velocities : $\overline{U}_{\infty,0} = [0.35; 0.45]$ m.s$^{-1}$. The flow fields, 50×60cm, captured the whole boundary layer depth and were centered at $x$= 0.09, 0.15, 1, 2.9, 6.1, 7.8 and 10.8m. The fluctuations ($u_i'$) are the difference between the raw field ($u_i$) and the spatially and temporally averaged field ($\overline{U_i}$) with 1000 computed velocity fields and 60 velocity vector columns per measured velocity field, i.e. 60000 samples.

## 3 Boundary layer development

### 3.1 Roughness parameters

Above the roughness layer and near the surface, $\overline{U}$ is expected to follow the log-law : $\frac{\overline{U}}{u_*} = \frac{1}{\kappa} ln\left(\frac{z-z_d}{z_0}\right)$, where $\kappa$ is the Von Karman's constant, fixed here at 0.4 and $z_d$ the displacement length, from which the coefficients can be computed. Here we choose to determine $u_*$ and $z_0$ independently by extrapolating $\overline{u'w'}$ at $z = z_d$. As expected, $u_*$ decreases with $x$ until quasi-asymptotic value is reached ; 1.8 × 10$^{-2}$m.s$^{-1}$ for $\overline{U}_{\infty,0}$=0.35 m.s$^{-1}$ and 2.4 × 10$^{-2}$m.s$^{-1}$ for $\overline{U}_{\infty,0}$=0.45 m.s$^{-1}$. The roughness length $z_0$, for both flow velocities was found to be approximately and asymptotically constant (2.5 × 10$^{-4}$m ± 5 × 10$^{-5}$m), as expected. These results confirm that the flow is fully turbulent within the canopy : $Re_* = \frac{z_h u_*}{\nu} = 170$ for $\overline{U}_\infty = 0.35 m.s^{-1}$ and 230 for $\overline{U}_\infty = 0.45 m.s^{-1}$.

### 3.2 Vertical development of the boundary layer

The height of the boundary layer, $\delta(x)$, has been determined via two methods : the height where $\overline{U}$ reaches 99% of the free-stream velocity ($\overline{U}_\infty$) and the height where the flux $\overline{u'w'}$ decreases to 5% of its maximum value. Both heights are in close agreement and the average of both estimations was used to fit the evolution of the boundary layer height, yielding :

$$\frac{\delta}{z_0}(\frac{x}{z_0}) = 0.18\,(\frac{x}{z_0})^{0.79} - 203\,. \tag{1}$$

This power law exponent is close to the classic theoretical $x^{4/5}$ power-law (Elliot, 1958).

### 3.3 Turbulent quantities

Figures 1-(a),(b),(c) show the profiles of $\overline{u'^2}/{u_*}^2$, $\overline{w'^2}/{u_*}^2$ and $\overline{-u'w'}/{u_*}^2$, respectively, as a function of $z/\delta$, for all the positive $x$ positions. The normalized intensity of these variances and covariances, at last initially, increases with $x$. Following the study of Antonia and Luxton (1971), the increase of $\overline{u'^2}/{u_*}^2$ is linked to the intensification of the vertical gradient of $\overline{U}$ which is accompanied with an increase of dynamical production. The equilibrium of all quantities is reached between stations 2.9m and 6 m.

$\overline{u'^2}/{u_*}^2$ and $\overline{-u'w'}/{u_*}^2$ are at maximum near the top of roughness elements due to the existence of turbulent structures which are generated by the roughness elements (Castro et al., 2006). From these maxima, $\overline{u'^2}/{u_*}^2$ decreases linearly up to the top of the outer layer. Figures 1-(a) and 2.(b) reveal that $\overline{w'^2}/{u_*}^2$ is about four times smaller than $\overline{u'^2}/{u_*}^2$, i.e. the flow is strongly anisotropic, in agreement with Grant (1986) who measured $\overline{u'^2}/\overline{w'^2} \sim 4$). The diminution of $\overline{-u'w'}/{u_*}^2$ is quasi-linear,as expected, with a change of slope near $z/\delta \sim 0.6$. Indeed, near the rough wall the intensity remains roughly constant as often observed for neutral boundary layer measurements (Cheng and Castro, 2002a and 2002b ; Chow et al., 2005 ; Drobinski et al. (2007)).

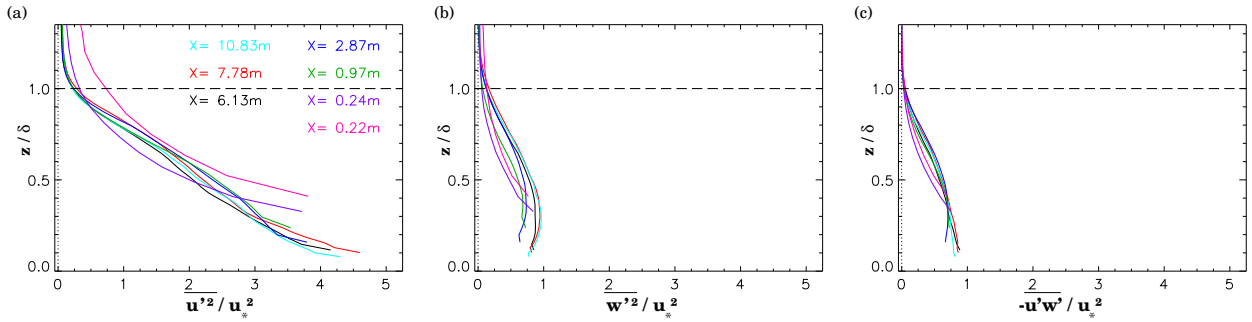


FIGURE 1 – Normalized profiles of $\overline{u'^2}/{u_*}^2$, $\overline{w'^2}/{u_*}^2$ and $\overline{u'w'}/{u_*}^2$ (respectively (a), (b) and (c)) as a function of $z/\delta$ for all positive measured $x$ positions.

## 4 Turbulent budgets

This section examines the budgets of the second-order turbulent transport equations to characterize the transfers between the turbulent quantities. The Reynolds-stress transport equation is given by Equation (2) where Coriolis and thermal production effects are not considered.

$$\frac{\partial}{\partial t}(\overline{u_i' u_j'}) = \underbrace{-\overline{U_k}\frac{\partial \overline{u_i' u_j'}}{\partial x_k}}_{ADV} \underbrace{-\left(\overline{u_k' u_i'}\frac{\partial \overline{U_j}}{\partial x_k} + \overline{u_k' u_j'}\frac{\partial \overline{U_i}}{\partial x_k}\right)}_{DP} \underbrace{-\frac{1}{\rho_0}\left(\overline{u_i'\frac{\partial p'}{\partial x_j}} + \overline{u_j'\frac{\partial p'}{\partial x_i}}\right)}_{PC}$$
$$\underbrace{-2\,\nu\,\overline{\left(\frac{\partial u_i'}{\partial x_k}\cdot\frac{\partial u_j'}{\partial x_k}\right)}}_{DISS} \underbrace{-\frac{\partial \overline{u_k' u_i' u_j'}}{\partial x_k}}_{TR} \underbrace{+\nu\,\frac{\partial^2 \overline{u_i' u_j'}}{\partial x_k \partial x_k}}_{DIFF} \qquad (2)$$

From left to right, the terms are : advection ($ADV$), dynamical production ($DP$), pressure-correlation ($PC$), dissipation ($DISS$), turbulent transport ($TR$) and molecular diffusion($DIFF$). The diffusion term can be neglected since it is the product of the viscosity ($10^{-6}$ m$^2$.s$^{-2}$) by second-order derivatives. The index $k$ ranges from 1 to 3 and refers respectively to the longitudinal, transverse and vertical component. For evaluating the turbulent kinetic energy, $e$, it is supposed that $\overline{v'^2} \sim 0.5(\overline{u'^2} + \overline{w'^2})$, with a coefficient being measured by Cheng et al. (2002b) and simulated by Castro et al. (2006). Under the present two-dimensional conditions, the transverse gradients ($\partial/\partial y$) of the time-averaged quantities and transverse mean velocity ($\overline{V}$) can also be neglected. Lastly, since the flow is statistically stationary, $\frac{\partial}{\partial t} = 0$.

### 4.1 Turbulent kinetic energy evolution

In addition to the above approximations, in the budget of the turbulent kinetic energy ($e$), the pressure-correlation term is neglected as it is expected to be a relatively weak transport term as for a smooth boundary layer (e. g., Pope, 2004). This implies :

$$PC_{\overline{u'^2}} + PC_{\overline{v'^2}} + PC_{\overline{w'^2}} \cong 0\,. \qquad (3)$$

Since the pseudo-dissipation term ($DISS$), $\tilde{\varepsilon}$, is the only unknown quantity of the measured budget of $e$, it will be the residual term. For 0m $< x <$ 2.87m and $0.7 > z/\delta > 0.3$, Figure 2-(a) shows that the development induces higher dynamical production : this "surplus" is balanced by an increase of the vertical turbulent transport of $e$. This result underlines that the equilibrium is reached in the region 2.9 m $< x <$ 6m, as already observed. For $x >$ 6m, above the surface layer ($z/\delta > 0.1$), advection is a minor term, comparable to the also minor vertical turbulent transport. However, the vertical turbulent transport is not negligible at the top of the outer layer for $1 > z/\delta > 0.6$ where it is the only source here. Thus, in the outer layer, the balance is roughly the same as for a smooth boundary layer. This agrees with the numerical results of Bhaganagar et al. (2004) who show that in this layer there are no significant difference, in support of Townsend's (1976) similarity hypothesis.

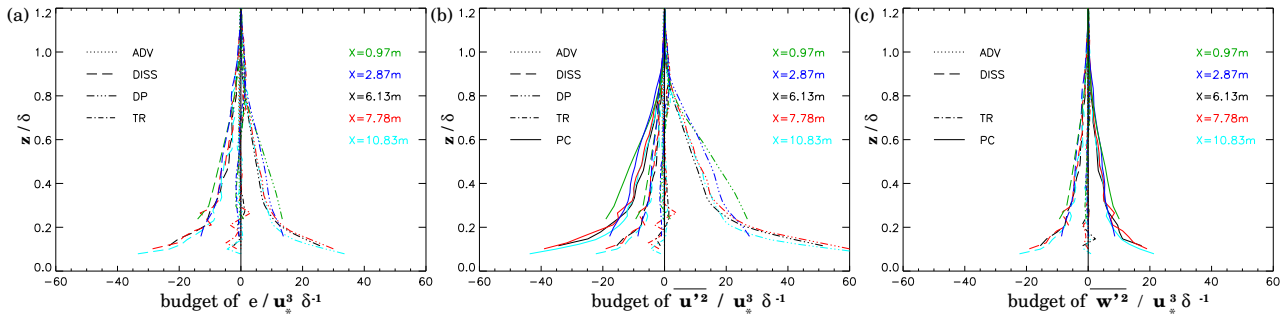


FIGURE 2 – Normalized budget of $e$, $\overline{u'^2}$, $\overline{w'^2}$ and $\overline{u'w'}$ (respectively (a), (b) and (c)) as a function of $z/\delta$ for all positive measured $x$ positions.

## 4.2 $\overline{u'^2}$ and $\overline{w'^2}$ evolution equation

The dissipation term ($\varepsilon_{ii}$) and the pressure-correlation ($PC$) term are the two unknown quantities of the measured budget $\overline{u_i'^2}$. Thus, an additional hypothesis needs to be made, where we invoke smooth-wall results : Pope (2004), for example, shows that for $z/\delta > 0.2$, there is approximate isotropy : $\varepsilon_{ij} = \frac{2}{3}\,\tilde{\varepsilon}\,\delta_{ij}$. Thus, the pressure-correlation is the only residual term of the budget of $\overline{u'^2}$ and $\overline{w'^2}$ and they can therefore individually and independently be estimated.

The $\overline{u'^2}$ budget (Figure 2-(b)) shows, as expected, that the turbulence acts principally in the lower part of the outer layer. Above the surface layer, the dynamical production is the only source as for a smooth boundary layer (Pope, 2004). The pressure-correlation term is the main sink (respectively, the main source) for $\overline{u'^2}$ (respectively, for $\overline{w'^2}$) above the surface layer. Similarly to boundary layers over a smooth surface, the pressure fluctuations appear to distribute the energy between the different components : from $\overline{u'^2}$ to $\overline{v'^2}$ and $\overline{w'^2}$ (Equation 3, which allows $PC_{\overline{v'^2}}$ to be evaluated). Figure 3 shows that the pressure fluctuations equitably distribute the energy contained in the longitudinal fluctuations to the transverse and vertical fluctuations. We also find that the equilibrium is reached between 2.9m and 6m.

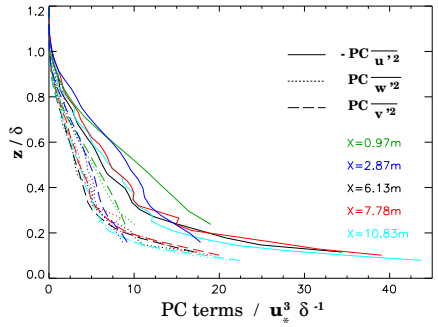


FIGURE 3 – Normalized magnitude of the pressure-correlation terms of $\overline{u'^2}$, $\overline{w'^2}$ and $\overline{v'^2}$ as a function of $z/\delta$ for all positive measured $x$ positions.

# 5 Integral length-scales and parameterization of the dissipative and mixing lengths

In this section, we investigate and parameterize the dissipative $l_\varepsilon$ and mixing $l_m$ lengths to model the Reynolds stresses in 1D prediction models. An accurate quantification of these turbulent length scales is essential as they mainly drive the development of the boundary layer. With the present measurements, there are three principal methods to determine the dissipative and mixing lengths which are both characteristic of the large scales. The first, indirect, yields the integral scales determined via spatial correlations. The second uses Taylor's estimation rate via the measured dissipation rate, and the third relies on the Boussinesq's model via the turbulent flux and the gradients of mean quantities. We consider here only the region where the flow has reached equilibrium, i.e for $x > 6$m.

The PIV measurements allow the spatial correlation function to be estimated directly. The integral length-scale is thus computed via the integral of the spatial auto-correlation functions $R_{\overline{u_i'u_j'},r}$ :

$$L_{\overline{u_i'u_j'},r}(z) = \int_{R=1}^{R=0.1} R_{\overline{u_i'u_j'},r}(\delta r)dr; \tag{4}$$

where $r$ is the longitudinal or vertical (respectively $x$ or $z$) direction and $\delta r$ the corresponding $x$ or $z$ displacement, which either positive or negative. This differs from the usual estimates based on temporal measurements using Taylor's hypothesis. We chose to analyze only the correlation with the vertical direction since transport in the vertical direction is the principal one.

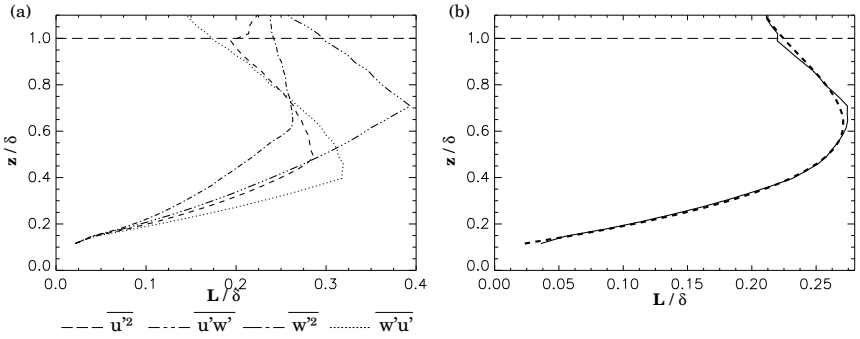


FIGURE 4 – (a) : Integral length normalized by $\delta$ for $\overline{u'^2}$ (dashed lines), $\overline{w'^2}$ (dash-dot lines), $\overline{u'w'}$ (dash-dot-dot-dot line) and $\overline{w'u'}$ (doted lines) following the vertical direction. (b) : Mean experimental integral length scale ($L$) (solid line) and its fit (dashed line).

Figure 4-(a) shows that these integral length-scales roughly have the same intensity. To parameterize the integral length-scale in 1D prediction models a representative integral length-scale ($L$) was taken as the average of the four vertical length scales. The mean integral length-scale ($L$) in Figure 4-(b) is linear in the lower part of the outer layer, as expected. Above, $L$ tends to be hyperbolic until the top of the outer layer. A function of the form $az/(b+z^k)$ fits this data :

$$\frac{L}{\delta} = \frac{A\left(\frac{z-z_h}{\delta} - s\right)}{B + \left(\frac{z-z_h}{\delta} - s\right)^p}, \tag{5}$$

with $A$=0.3 ; $s$=0.03 ; $p$=2 and $B$=0.31. The maximum value reached is $L/\delta \sim 0.26$ at $z/\delta = 0.7$.

Using the dissipation rate obtained from the budget of $e$, the dissipative length ($l_\varepsilon$) can be determined : $\tilde{\varepsilon} = C_\varepsilon \frac{e^{3/2}}{l_\varepsilon}$, $C_\varepsilon$ is a constant largely fixed at 0.845 (Cheng et al. 2002). Figure 5-(a) shows that except in the region near the surface ($z/\delta$ <0.3) where the hypothesis of isotropy is not verified and at the top of the outer layer ($z/\delta$ >0.8) where $e$ becomes small, the coefficient of proportionality $C = l_\varepsilon/L$ is roughly constant and about 2.4. Thus, as a first approximation in accordance with standard modeling practices, the integral length-scale $L$ can be used to parameterize the dissipation rate as :

$$\tilde{\varepsilon} = C_\varepsilon \frac{e^{3/2}}{C\,L} \sim 0.35\frac{e^{3/2}}{L}. \tag{6}$$

Similarly, $l_m^2 = -\frac{\overline{u'w'}}{\partial\overline{U}/\partial z}$ was computed. For $z/\delta$ >0.6, it reaches $l_m/\delta$ ~0.08 before growing exponentially, as $z/\delta$ =1 is approached, as expected. Figure 5-(b) shows that, $l_m$ normalized by $L$ ($l_m/L$) roughly equals to 0.36 between $0.2 < z/\delta < 0.8$. Thus, as a first approximation : $l_m \sim 0.36L$.

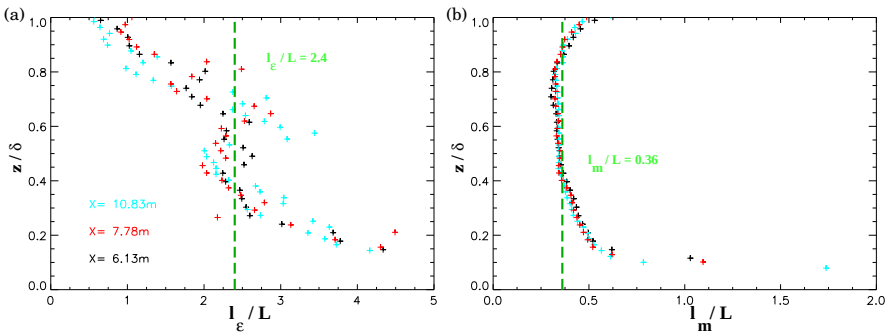


FIGURE 5 – (a) Ratio of the integral length scale and the dissipative length ($l_\varepsilon/L$) at several $x$ positions as a function of $z/\delta$. (b) Ratio of the integral length scale and the dissipative length ($l_m/L$) at several $x$ positions as a function of $z/\delta$.

# 6 Conclusion

The evolution of the boundary layer developing over a rough surface has been described in terms of the turbulent statistics and their budets. The results show that equilibrium is reached at $x/z_0 \sim 2 \times 10^4$ for all quantities. Their behavior at equilibrium is in agreement with smooth wall equivalent, indicating that Towsend's Reynolds number similarity is observed at high Reynolds and low roughness blockage ratios.
The main advantage of the new relation (5) is that it can be used in the neutral case where there is not a gradient of temperature (in comparison with old formulation which relies on the gradient of temperature within the outer layer (Bougeault and Lacarrère (1989))). If $\delta$ can not be directly estimated, the height where the Reynolds stresses become zero can be used. The relation (5) can be considered as an improvement for modeling the mixing and dissipative length scales. Further numerical tests need to be done in order to validate these proposal.

# 7 Acknowledgements

We thank B. Beaudoin, J-C. Boulay, J.-C. Canonici, M. Morera, S. Lassus Pigat and H. Schaffner of the CNRM-GAME fluid mechanics laboratory (SPEA) for their support during the experiments.

# Références

[1] Townsend A. A. The structure of turbulent shear flow. Cambridge University Press, 1976. pp. 152-154.

[2] Antonia R. A. and Krogstad P. A. Turbulence structure in boundary layer over different type of surface roughness. Fluid Dyn. Res., 28, 139–157, 2001.

[3] Coceal O., Thomas T. G., Castro I. P., and Belcher S. E. Mean flow and turbulence statistics over groups of urban-like cubical obstacle. Bound.-Layer Meteor., 121(3), 475–490, 2006.

[4] Jiménez J. Turbulent flows over rough walls. Ann. Rev. Fluid Mech., 36, 173–196, 2004.

[5] Schultz M. P. and Flack K. A. The rough-wall turbulent boundary layer from the hydraulically smooth to the fully rough regime. J. Fluid. Mech., 580, 381–405, 2007.

[6] Castro I. P. Rough-wall boundar layers : mean flow universality. J. Fluid. Mech., 585, 469–485, 2007.

[7] Macdonald R. W. Modelling the mean velocity profile in the urban canopy layer. Bound.-Layer Meteor., 97, 25–45, 2000.

[8] Elliott W. The growth of the atmospheric internal boundary layer. Trans. Am. Geophys. Un., 39, 1048–1054, 1958.

[9] Antonia R. A. and Luxton R. E. The response of a turbulent boundary layer to a step change in surface roughness. part 1. smooth to rough. J. Fluid. Mech., 48, 721–761, 1971.

[10] Castro I. P., Cheng H., and Reynolds R. Turbulence over urban-type roughness : deductions from wind-tunnel measurements. Bound.-Layer Meteor., 118, 109–131, 2006.

[11] Grant A. L. M. Observations of boundary layer structure made during the 1981 kontur experiment. Q. J. Roy. Meteor. Soc., 112, 825–841, 1986.

[12] Cheng H. and Castro I. P. Near-wall flow development after a step change in surface roughness. Bound.-Layer Meteor., 105, 411–432, 2002a.

[13] Cheng H. and Castro I. P. Near-wall flow over urban-like roughness. Bound.-Layer Meteor., 104, 229–259, 2002b.

[14] Chow F. K., Street R. L., Xue M., and Ferziger J. H. Explicit filtering and reconstruction turbulence modeling for large-eddy simulation of neutral boundary layer flow. J. Atmos. Sci., 62, 2058–2077, 2005.

[15] Drobinski P., Carlotti P., Redelsperger J. L., Banta R. M., Masson V., and Newson R. K. Numerical and experimental investigation of the neutral atmospheric surface layer. J. Atmos. Sci., 64, 137–156, 2007.

[16] Pope S. B. Turbulent Flows. Cambridge University Press, 2004. 183-188pp, 273-275pp, 298-308pp, 313-318pp, 369-371pp.

[17] Bhaganagar K., Kim J., and Coleman G. Effect of roughness on wall-bounded turbulence. Flow Turbulence Combust., 72, 463–492, 2004.

[18] Cheng Y., Canuto V. M., and Howard A. M. An improved model for the turbulent pbl. J. Atmos. Sci., 59, 1550–1565, 2002.

[19] Bougeault P. and Lacarrère P. Parameterization of orography-induced turbulence in a meso-beta scale model. Mon. Wea. Rev., 117, 1870–1888, 1989.